Stem Cell Research 41 (2019) 101631

Contents lists available at ScienceDirect

Stem Cell Research

journal homepage: www.elsevier.com/locate/scr

Generation of a genetically modified human embryonic stem cells expressing fluorescence tagged ATOX1

Meng-Hsuan Wen[a], Xihong Xie[a], Jian Tu[b,c], Dung-Fang Lee[b,d,e,f], Tai-Yen Chen[a,*]

[a] Department of Chemistry, University of Houston, Houston, Texas 77204, United States
[b] Department of Integrative Biology and Pharmacology, McGovern Medical School, The University of Texas Health Science Center at Houston, Houston, TX 77030, United States
[c] Department of Musculoskeletal Oncology, The First Affiliated Hospital of Sun Yat-sen University, Guangzhou 510080, China
[d] The University of Texas MD Anderson Cancer Center UTHealth Graduate School of Biomedical Sciences, Houston, TX 77030, USA
[e] Center for Stem Cell and Regenerative Medicine, The Brown Foundation Institute of Molecular Medicine for the Prevention of Human Diseases, The University of Texas Health Science Center at Houston, Houston, TX 77030, United States
[f] Center for Precision Health, School of Biomedical Informatics, The University of Texas Health Science Center at Houston, Houston, TX 77030, United States

A B S T R A C T

ATOX1 is a copper chaperone involved in intracellular copper homeostasis, cell proliferation, and tumor progression. To investigate the physiologically relevant molecular mechanism of ATOX1 by using imaging-based approaches, we genetically modified ATOX1 in H1 hESCs to express mCherry-ATOX1 fusion protein under endogenous regulatory machinery. The fluorescence engineered hESC clone maintains characteristic stem cell features and can differentiate to all three germ layers, serving as a unique tool to dissect the role of ATOX1 in various cellular processes.

Resource Table

Unique stem cell lines identifier	WAe001-A-29
Alternative names of stem cell lines	H1_mCh-ATOX1 (KI) / UHMCe002-A-29
Institution	University of Houston, Houston, TX, United States
Contact information of distributor	Tai-Yen Chen (tchen37@central.uh.edu)
Type of cell lines	ESC
Origin	Human embryonic stem cell line
Additional origin info	Age: N/ASex: Male Ethnicity if known: N/A
Cell Source	H1 hESCs
Clonality	Clonal
Method of reprogramming	N/A
Gene modification	Yes
Type of modification	Transgene expression (fluorescence protein)
Associated disease	N/A
Gene/locus	5q33.1; ATOX1 exon 2
Method of modification	CRISPR
Name of transgene or resistance	mCherry
Inducible/constitutive system	N/A
Date archived/stock date	5/18/2019
Cell line repository/bank	https://hpscreg.eu/cell-line/WAe001-A-29
Ethical approval	Cell lines were used according to institutional guidelines. UTHealth approval number: SCRO–16–01

1. Resource utility

We have engineered the ATOX1 exon 2 in a H1 human embryonic stem cell line to express mCherry-ATOX1 fusion proteins. This cell line can differentiate to different germ layers, which is useful for imaging-based studies on molecular mechanisms of ATOX1.

2. Resource details

ATOX1 is an intracellular copper chaperone, a cell-cycle modulator, and a therapeutic cancer target (Celauro, Mukaj, Fierro-Gonzalez, and Wittung-Stafshede, 2017; Hamza et al., 2001; Matson Dzebo, M., S., S., and E., 2018). ATOX1 deficiency results in perturbed intracellular trafficking of copper transporters and altered cell proliferation during early development. ATOX1 is ubiquitously observed in different cells and tissues. However the detail intracellular molecular behaviors, such as subcellular distribution and interaction dynamics, of ATOX1 in response to environmental cues are still unclear. To dissect the roles of ATOX1 in different cell contexts under endogenous regulatory by using

* Corresponding author.
E-mail address: tchen37@central.uh.edu (T.-Y. Chen).

https://doi.org/10.1016/j.scr.2019.101631
Received 24 August 2019; Received in revised form 26 September 2019; Accepted 14 October 2019
Available online 16 October 2019

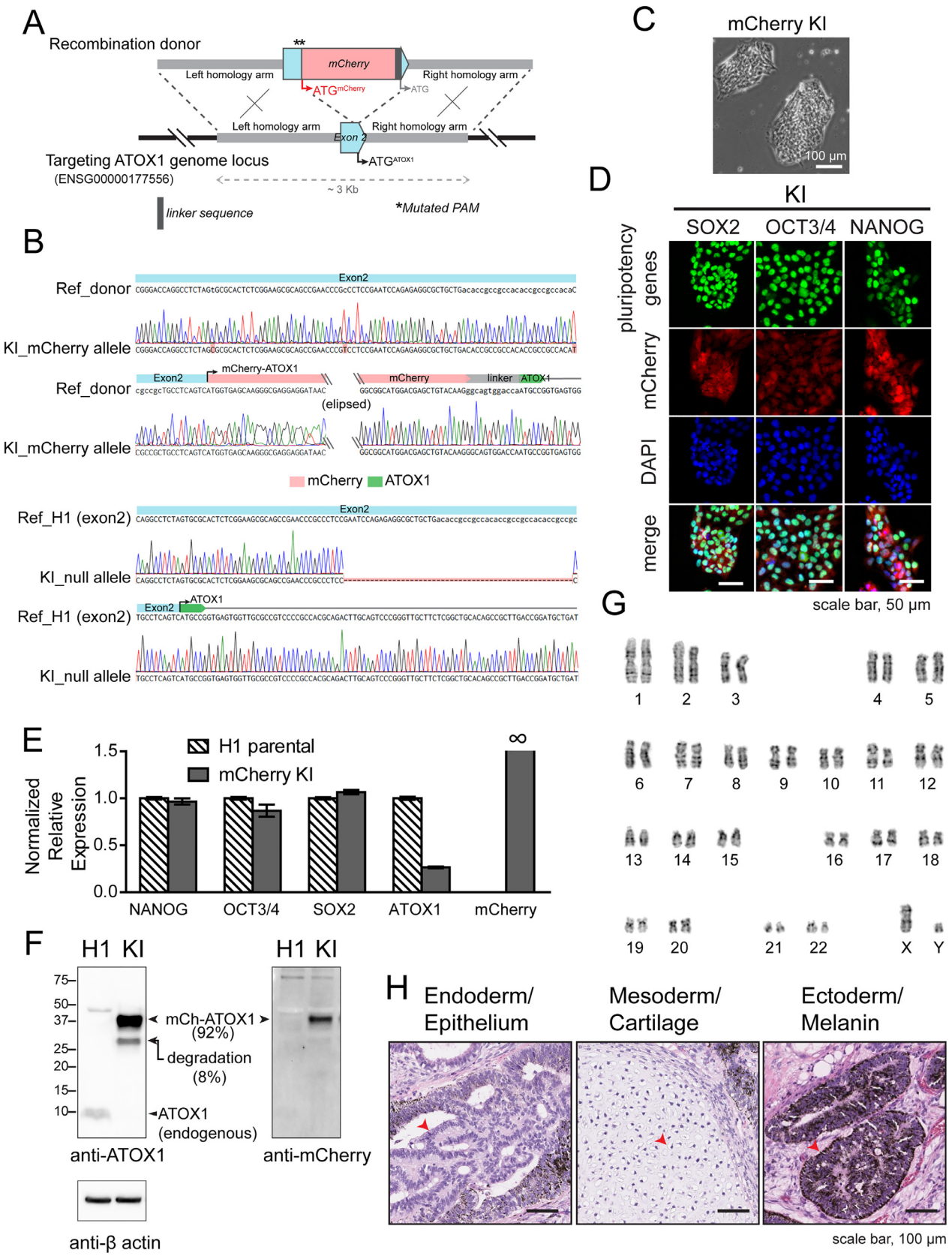
A
Recombination donor
**
mCherry
Left homology arm
Right homology arm
ATG mCherry
ATG
Left homology arm
Right homology arm
Exon 2
ATG ATOX1
Targeting ATOX1 genome locus
(ENSG00000177556)
~ 3 Kb
linker sequence
*Mutated PAM
B
Ref_donor
Exon2
KI_mCherry allele
mCherry-ATOX1
mCherry
linker
ATOX1
(elipsed)
mCherry
ATOX1
Ref_H1 (exon2)
KI_null allele
C
mCherry KI
100 μm
D
KI
SOX2
OCT3/4
NANOG
pluripotency genes
mCherry
DAPI
merge
scale bar, 50 μm
E
H1 parental
mCherry KI
Normalized Relative Expression
1.5
1.0
0.5
0.0
∞
NANOG
OCT3/4
SOX2
ATOX1
mCherry
F
H1 KI
H1 KI
75
50
37
25
20
15
10
mCh-ATOX1 (92%)
degradation (8%)
ATOX1 (endogenous)
anti-ATOX1
anti-mCherry
anti-β actin
G
1 2 3 4 5
6 7 8 9 10 11 12
13 14 15 16 17 18
19 20 21 22 X Y
H
Endoderm/ Epithelium
Mesoderm/ Cartilage
Ectoderm/ Melanin
scale bar, 100 μm

Fig. 1.

Table 1
Characterization and validation.

Classification	Test	Result	Data
Morphology	Photography	Normal	Fig. 1 panel C
Phenotype	Qualitative analysis: Immunocytochemistry	Positive staining for pluripotency factors NANOG, OCT3/4, and SOX2	Fig. 1 panel D
	Quantitative analysis: RT-qPCR	Comparable expression levels of NANOG, OCT3/4, and SOX2 compared with H1	Fig. 1 panel E
Genotype	Karyotype (G-banding) and resolution	46XY; Resolution 450–500	Fig. 1 panel G
Identity	Microsatellite PCR (mPCR) OR	N/A	N/A
	STR analysis	8 sites tested; all sites match parental H1	Data available with authors
Mutation analysis (IF APPLICABLE)	Sequencing	Heterozygous insertion	Fig. 1 panel B and Supplementary figure 2
	Southern Blot	Tag insertion in one allele, small deletion in the other allele, no apparent off-target effect	Supplementary figure 1
Microbiology and virology	Mycoplasma	Mycoplasma test shows negative	Supplementary figure 3
Differentiation potential	Teratoma formation	Differentiation to three germ layers confirmed by H&E staining	Fig. 1 panel H
Donor screening (OPTIONAL)	HIV 1 + 2 Hepatitis B, Hepatitis C	N/A	N/A
Genotype additional info (OPTIONAL)	Blood group genotyping	N/A	N/A
	HLA tissue typing	N/A	N/A

single-molecule super-resolution microscopy in live cell (Chen et al., 2015), here we genetically tagged ATOX1 with fluorescence protein in the H1 stem cell to generate the mCherry-ATOX1 knocked-in (H1_mCh-ATOX1, KI) clone.

We genetically modified H1 human embryonic stem cells (hESCs) by CRISPR-Cas9 mediated homologous recombination (Fig. 1A). H1 hESCs were co-transfected with the single-guide RNAs (sgRNAs)-Cas9 containing plasmids together with corresponding recombination donor plasmids. After puromycin selection, the emerged hESC clones were picked and screened for mCherry insertion by Southern blotting (Suppl. Fig. 1) and DNA sequencing. We obtained a heterozygous mCherry-ATOX1 KI clone: One allele carries mCherry in-framed insertion upstream to the ATOX1 start codon, yet the other allele has a 51 bp deletion at −12 to the ATOX1 start codon and no mCherry insertion (Fig. 1B & Suppl. Fig. 2). Nevertheless, the deletion has no overt impacts because the KI clone still grows normally and exhibits characteristic hESC morphology (i.e., densely packed cell clusters with well-defined borders, Fig. 1C). This KI clone is free of mycoplasma contamination tested by PCR-based method (Table 1). Immunofluorescence staining demonstrated expression of pluripotency transcription factors NANOG, OCT3/4, and SOX2 in KI clone (Fig. 1D). We further quantified the transcription of pluripotency genes, ATOX1, and mCherry by qRT-PCR (Fig. 1E). Compared with the parental H1 hESCs, KI cells showed comparable expression of all three pluripotency genes (NANOG, 97 ± 3%; OCT4, 87 ± 6%; and SOX2, 107 ± 2%), but the level of ATOX1 transcript in KI clone was reduced (26 ± 1%). Despite the reduced transcript level, immunoblotting results against ATOX1 showed increased mCherry-ATOX1 protein level in the KI lysate compared to the endogenous ATOX1 in the parental H1 lysates (Fig. 1F), probably due to improved protein stability. The un-tagged ATOX1, expected to be endogenous ATOX1 expressed from mCherry-null allele, was barely detectable in the KI hESC lysate, suggesting that endogenous ATOX1 was effectively knocked out in the mCherry-null allele. G-band karyotype analysis confirmed the normal karyotype of KI hESCs (Fig. 1G). Histological staining of KI hESC-derived teratoma showed characteristics of epithelium (endoderm), cartilage (mesoderm), and melanin (ectoderm), confirming the differentiation capability of KI hESCs to three germ layers (Fig. 1H). The short tandem repeat (STR) profile also confirmed that the KI cell still maintains its identity to the parental H1 hESCs (data available upon request). The characterization of KI hESCs is summarized in Table 1.

In summary, the fluorescence KI hESC clone is pluripotent and possesses normal karyotypes. With fluorescence protein mCherry directly tagged on ATOX1 whose expression is still controlled by endogenous regulatory machinery, KI hESCs enable imaging-based approaches to study the cell-type-specific function of ATOX1.

3. Materials and methods

3.1. Cell culture

H1 hESCs (NIH Registration Number: 043, WiCell, passage 28–30) were maintained in mTeSR™1/Matrigel™ feeder-free system at 37 °C with 5% CO2 until cells reach 80% confluent. Cells were genetically engineered via CRISPR/Cas9 mediated homologous recombination by co-electrotransfecting sgRNA-Cas9 plasmids and homology-direct recombination (HDR) donor plasmid. Transfected cells were plated on puromycin-resistant MEF feeders overnight followed by puromycin selection for four days. Clones were picked and seeded in plates under feeder-free culture system again then passaged for clonal expansion and characterization.

3.2. CRISPR plasmid design

We adopted the protocol from Ran et al. (Ran et al., 2013) and designed the sgRNAs using web tool from Benchling. The sgRNAs targeting to the upstream of ATOX1 coding region (Table 2) were cloned into the pSpCas9(BB) − 2A-Puro (PX459) V2.0 plasmid (Addgene). A 3 kb genome region covering ATOX1 exon 2 (NC_000005.10, 151,757,164..151760261) were PCR amplified from H1 genome and cloned into pMiniT2 plasmid (NEB) as HDR arm. The mCherry sequence was PCR amplified and assembled into the donor plasmid by seamless cloning (NEB).

3.3. PCR, sequencing, and str

Genomic DNA was isolated from ~2 × 106 cells by using MasterPure™ Complete DNA and RNA Purification Kit (Epicentre). PCR was performed using primers (Table 2) and AccuStart™ II GelTrack PCR SuperMix (QuantaBio). PCR protocol: 95 °C for 3 min; 25 cycles of 95 °C for 30 s, 60 °C for 10 s, and 68 °C for 3.5 min; and 72 °C for 5 min. Sanger sequencing was performed by Eton Bioscience. STR DNA fingerprinting was done by the CCSG-funded Characterized Cell Line Core Facility (The University of Texas M.D. Anderson Cancer Center). The STRs at 8 loci were assessed.

3.4. qRT-PCR

Total RNA was isolated the same way as DNA. Two microgram of total RNA were converted to cDNA by using All-in-One RT MasterMix

Table 2
Reagents details.

Antibodies used for immunocytochemistry/immunoblotting			
	Antibody	Dilution	Company Cat # and RRID
Pluripotency Markers	Goat anti-NANOG	1:500 (ICC)	R&D Systems Cat# AF1997 RRID: AB_355,097
	Mouse anti-OCT3/4	1:250 (ICC)	Santa Cruz Biotechnology Cat# sc-9081, RRID:AB_2,167,703
	Goat anti-SOX2	1:250 (ICC)	Santa Cruz Biotechnology Cat# sc-17,320, RRID:AB_2,286,684
Characterization Markers	Rabbit anti-mCherry	1:500 (ICC) 1:1000 (IB)	Abcam Cat# ab167453, RRID:AB_2,571,870
	Rabbit anti-ATOX1	1:1000 (IB)	Abcam Cat# ab154179 RRID:
	Mouse anti- β Actin	1:2000 (IB)	Sigma-Aldrich Cat# A5441, RRID:AB_476,744
Secondary antibodies	Donkey anti-Goat IgG (Alexa Fluor488 conjugate)	1:1000 (ICC)	Jackson ImmunoResearch Labs Cat# 705–545–003, RRID:AB_2,340,428
	Donkey anti-Mouse IgG (Alexa Fluor488 conjugate)	1:1000 (ICC)	Thermo Fisher Scientific Cat# A-21,202, RRID:AB_141,607
	Donkey anti-Rabbit IgG (Alexa Fluor594 conjugate)	1:1000 (ICC)	Thermo Fisher Scientific Cat# A-21,207, RRID:AB_141,637
	Peroxidase-AffiniPure Goat Anti-Mouse IgG	1:10,000 (IB)	Jackson ImmunoResearch Labs Cat# 115–035–003, RRID:AB_10,015,289
	Peroxidase-AffiniPure Goat Anti-Rabbit IgG	1:10,000 (IB)	Jackson ImmunoResearch Labs Cat# 111–035–045, RRID:AB_2,337,938

Primers		
	Target	Forward/Reverse primer (5′ − 3′)
CRISPR Plasmid 1 (sgRNA)	ATOX1	CACCAGCGCCTCTCTGGATTCGGA/ AAACTCCGAATCCAGAGAGGCGCT
CRISPR Plasmid 2 (sgRNA)	ATOX1	CACCGGGCATGACTGAGGCAGCGG/ AAACCCGCTGCCTCAGTCATGCCC
HDR Genome	ATOX1 intron 1–2	TTCCTTCAGCTGTTATCTTGTGGTA/ ACTTTTCACTGTACGCTACTTTGTG
Site direct mutagenesis	PAM of ATOX1 sgRNA 1	GCCGAACCCGTCCTCCGAATC/ TGCGCTTCCGAGAGTGCG
Site direct mutagenesis	PAM of ATOX1 sgRNA 2	CGCCGCCACATCGCCGCTGCC/ GTGTGGCGGCGGTGTCAGCAGC
Donor Plasmid Assembly	ATOX1-mCherry	GCATTCCCTAACACAAGCTTGAC/ GACTGAGGCAGCGGCGATGTGG
Donor Plasmid Assembly	mCherry	GCTGCCTCAGTCATGGTGAGCAAG/ TGGTCCACTGCCCTTGTACAGCTCGTCCATG
Donor Plasmid Assembly	mCherry-ATOX1	GGCAGTGGACCAATGCCGGTGAGTG/ AGACGCACATGCGGCCGCCTCGAG
Pluripotency Markers (qPCR)	NANOG	TTTGTGGGCCTGAAGAAAACT/ AGGGCTGTCCTGAATAAGCAG
Pluripotency Markers (qPCR)	OCT4	AACCTGGAGTTTGTGCCAGGGTTT/ TGAACTTCACCTTCCCTCCAACCA
Pluripotency Markers (qPCR)	SOX2	AGAAGAGGAGAGAGAAAGAAAGGGAGAGA/ GAGAGAGGCAAACTGGAATCAGGATCAAA
Target mutation analysis (qPCR)	ATOX1	CATGCCGAAGCACGAGTT/ CTTCAGGGTTGCAAGCAGAG
Target mutation analysis (qPCR)	mCherry	CCCCGTAATGCAGTGTCGT/ CTCTGCTTGATCTCGCCCTT
House-Keeping Genes (qPCR)	GAPDH	CCACTCCTCCACCTTTGAC/ ACCCTGTTGCTGTAGCCA
Genotyping	ATOX1 exon 2	GGGCCCTTTCAGCTCAGAAT/ GTGTGACTGCTTTTGCCTGG

(Applied Biological Materials Inc). qPCR was performed using primers (Table 2) following the protocol of iQ SYBR Green Supermix (BioRad). Results were calculated using the ΔΔCT method and normalized to GAPDH expression.

3.5. Immunoblotting and immunofluorescence staining

An equal amount of total protein from cell lysate was resolved in a SDS-PAGE for immunoblotting analysis. For immunofluorescence staining, cells were fixed with 4% paraformaldehyde in PBS for 15 min, blocked and incubated with primary antibodies (Table 2) overnight at 4 °C, incubated with secondary antibodies, and counterstained with DAPI.

3.6. Karyotyping

The cultures were harvested and G-banded using standard protocols. Clonal chromosomal changes identified by G-banding were described according to an International System for Human Cytogenetic Nomenclature ISCN (McGowan-Jordan & An, n.d.). Twenty metaphase chromosome spreads at 400 band resolution were analyzed.

3.7. Teratoma assay

Cells grown under log-phase were dissociated and resuspended in 50% Matrigel/DMEM-F12. Immunodeficient NOD SCID mice (Charles River Laboratories) were injected subcutaneously with 2 × 107 cells in each flank and observed for palpable teratoma formation. After six weeks, teratomas were excised then fixed in 10% formalin (Sigma). Histology was analyzed using H&E staining.

3.8. Mycoplasma testing

Mycoplasma detection was performed using PCR Mycoplasma Detection Kit (Applied Biological Materials Inc.) according to the instructions from manufacturer

Declaration of Competing Interest

The authors declare no conflict of interest.

Acknowledgements

T.-Y.C. is supported by Welch Foundation (E-1947), NIH (R35GM133505), and University of Houston. D.-F.L. is supported by Rolanette and Berdon Lawrence Award in Bone Disease Program of Texas (60511) and CPRIT (RR160019).

Supplementary materials

Supplementary material associated with this article can be found, in the online version, at doi:10.1016/j.scr.2019.101631.

References

Celauro, E., Mukaj, A., Fierro-Gonzalez, J.C., Wittung-Stafshede, P., 2017. Copper chaperone ATOX1 regulates pluripotency factor OCT4 in preimplantation mouse embryos. Biochem Biophys Res Commun 491, 147–153.

Chen, T.-Y., Santiago, A.G., Jung, W., Krzemiński, Ł., Yang, F., Martell, D.J., Helmann, J.D., Chen, P., 2015. Concentration-and chromosome-organization-dependent regulator unbinding from dna for transcription regulation in living cells. Nat Commun 6, 7445.

Hamza, I., Faisst, A., Prohaska, J., Chen, J., Gruss, P., Gitlin, J.D., 2001. The metallochaperone atox1 plays a critical role in perinatal copper homeostasis. Proc Natl Acad Sci U S A 98, 6848–6852.

Dzebo, Matson, M., Blockhuys, S., Valenzuela, S., Celauro, E., Esbjorner, E.K., Wittung-Stafshede, P., 2018. Copper chaperone atox1 interacts with cell cycle proteins. Comput Struct Biotechnol J. 16, 443–449.

Ran, F.A., Hsu, P.D., Wright, J., Agarwala, V., Scott, D.A., Zhang, F., 2013. Genome engineering using the CRISPR-Cas9 system. Nat Protoc 8, 2281–2308.